コンクリート工学年次論文集, Vol.29, No.1, 2007

- Technical Paper -

FRACTURE ENERGY OF HYBRID FIBER REINFORCED HIGH STRENGTH CONCRETE UNDER HIGH TEMPERATURE CONDITION

Sofren L. SUHAENDI*1, Kazuo WATANABE*2, Kazunori SHIMURA*3 and Takashi HORIGUCHI*4

ABSTRACT

Addition of polypropylene fiber was found to be effective in mitigating explosive spalling, a catastrophic failure mechanism inconsistently observed when high strength concrete was exposed to high temperature condition. However, melting of these fibers would degrade the properties of high strength concrete surviving from explosive spalling. Hybrid fibers were developed to mitigate explosive spalling and maintain the properties of heated high strength concrete. This paper presents the effect of hybrid fibers on fracture energy of high strength concrete after heat exposition.

Keywords: high strength concrete, high temperature, hybrid fiber, fracture energy

1. INTRODUCTION

In spite of its superior performance, high strength concrete (HSC) was prone to catastrophic failure mechanism, termed as explosive spalling, under elevated temperature condition [1]. Some papers reported that this type of failure mechanism was closely related to the low permeability property of HSC. During exposition to high temperature, denser matrix of HSC would prevent water vapor escaping quickly. As temperature increased, this water vapor was accumulated inside the concrete matrix and build-up of a significant pore pressure was generated. Once the accumulation of pore pressure exceeds HSC tensile strength, it would spall in an explosive manner.

Other possible factor causing explosive spalling of HSC exposed to high temperature was thermal incompatibility between coarse aggregate and hardened cement paste (hcp). During exposition to high temperature, coarse aggregate would tend to expand while hcp would tend to shrink. This incompatibility would induce build-up of strain energy that might play a secondary role in explosive spalling mechanism [2].

Recent development in mitigating explosive spalling failure mechanism was achieved by the addition of short organic fibers, such as polypropylene fibers, into HSC mixture [3]. The melting of this type of fibers would create passages for the reduction of pore pressure inside the concrete matrix when HSC was exposed to high temperature. However, effectiveness in explosive spalling mitigation and residual behavior of HSC surviving high temperature exposition would closely depend on fiber geometry [4]. As optimization of polypropylene fibers had been comprehended, addition of polypropylene fibers into HSC mixture in this experimental study followed the optimum fiber geometry and composition from previous study.

Japan Concrete Institute (JCI) characterizes fracture parameter, fracture energy G_F, by the application of three-point bending test on center-notched beams. Fracture energy was then calculated adopting load–CMOD response from the test since this curve resembled several advantages compared to load–displacement response [5]. Hence, discussions in this paper were solely done using load-CMOD response.

Upon high temperature exposition, two different scenarios need to be assessed, during elevation of temperature and after high temperature exposition. The concept of hybrid fibers addition on HSC under high temperature condition is to achieve a synergy between polypropylene fibers and steel fibers. During elevation of temperature, polypropylene fibers are

*1 Doctor student, Dept. of Civil Engineering, Hokkaido University, MSc., M.E., JCI Member
*2 Master student, Dept. of Civil Engineering, Hokkaido University, JCI Member
*3 Research Associate, Dept. of Civil Engineering, Hokkaido University, Dr.E., JCI Member
*4 Associate Prof., Dept. of Civil Engineering, Hokkaido University, Dr.E., JCI Member

utilized to prevent explosive spalling while steel fibers are utilized to maintain mechanical properties in the aftermath of high temperature exposition. Present experimental study tried to investigate the effect of hybrid fibers on fracture behavior of HSC after heat exposition.

2. EXPERIMENT

2.1 Materials

(1) Short fibers

Two types of short fibers were utilized in the experimental study, namely polypropylene (PP) and steel fiber. Like mentioned earlier, geometry of PP fiber were decided in relation to the result from previous experimental study. As for steel fibers, two different geometry of this type of fibers were investigated. The properties of short fibers are shown in Table 1.

Table 1 Short fiber properties

Property	PP	Steel	
Length (mm)	6	13	30
Denier (D)	2.2	–	
d_{eff} (μm)	18	160	600
l/d	333	82	50
Shape	Fibrillated	Straight	Hooked ends
Density (kg/m^3)	900	7800	
T_{melt} ($^\circ$C)	160-170	1370	
$T_{vaporize}$ ($^\circ$C)	341	–	

(2) Concrete specimens

All series of concrete mixture were cast using ordinary portland cement, river sand, and crushed limestone. Fineness modulus of fine aggregate was 2.9 and maximum nominal size of coarse aggregate was 13 mm. Some mixing design parameters were kept constant: W/C of 0.3, sand to aggregate ratio (s/a) of 50%, and water content of 170 kg/m^3. Short fibers were added inside the concrete mixture as shown in Table 2. Some chemical admixtures: polycarboxylate-based superplasticizer, air entraining, and bubble cutter agent, were used to attain desired workability (slump of 150±25 mm) and air content (3±1%) of fresh concrete.

Beam specimens of 400×100×100 mm (L×B×D) in size were cast and cured under lime-saturated water at temperature of 20±2 $^\circ$C for 28 days. Before the bending test was performed, beam specimens were cut using a diamond saw to provide a central notch with a depth of 30 mm and a width of 4 mm. Soon, the specimens were stored inside a keeping room (T= 20 $^\circ$C and RH= 60%) for a couple of days.

Table 2 Fiber volume fraction

I.D.	Volume fraction (%)			
	PP	Steel		Total
	6 mm	13 mm	30 mm	
Plain	0		0	0
P6		0		0.1
Hy1	0.1		0.3	0.4
Hy2		0.1	0.2	0.4

Then, some specimens were heated inside a computer-controlled electric furnace. Heating rate was set at 10 $^\circ$C per minute with maximum temperature kept at 200, 400, and 600 $^\circ$C for two hours. Preventing thermal cracking upon cooling, heated specimens were let to cool inside the furnace until its temperature coincided with room temperature.

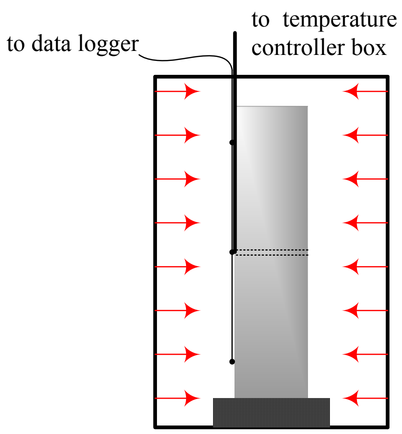

Fig. 1 Thermocouple settings

2.2 Experimental Method

(1) Loading and non-destructive test

In order to fully utilize concrete specimens, compressive strength test was performed on each one half of a broken beam according to JIS A 1108, setting the loading rate at 250 kPa/s. A commercial non-destructive test measurement, PUNDIT, was adopted to measure ultrasonic pulse velocity (UPV) of concrete specimens. Readings were performed on transversal direction applying frequency of 200 kHz.

(2) Bending test

Three point bending test of beam specimens were performed according to JCI-S-001-2003 or JCI-S-002-2003. A closed-loop testing machine with a maximum capacity of 200 kN was utilized to assure the test being conducted under displacement rate of about 5μm/s. Prior to loading, specimen was preloaded (~0.2 kN) to ensure good contact between loading platen and beam specimen.

The fracture energy G_F, defined as the total energy dissipated over the unit crack area, was obtained using the work done by the force (the area under a complete L–CMOD curve in three point bending, W_0) and the work done by the self-weight of the beam (W_1). Due to longer tail of L–CMOD curves on fiber reinforced concrete until breaking of specimen ($CMOD_c$), another toughness parameter (T^{CMOD2} and T^{CMOD4}) were introduced. T^{CMOD2} and T^{CMOD4} are defined as toughness until CMOD reaches 2 mm and 4 mm respectively, given beam depth (D) of concrete specimen to be equal to 100 mm. Calculation of fracture energy is done as follows:

$$G_F^{CMOD} = \frac{0.75W_0 + W_1}{A_{lig}}, \quad W_1 = 0.75\left(\frac{S}{L}m_1 + 2m_2\right)g.CMOD_c \tag{1}$$

$$T^{CMOD2} = \frac{0.75W_{CMOD2} + W_1}{A_{lig}}, \quad W_1 = \frac{0.75}{2}\left(\frac{S}{L}m_1 + 2m_2\right)g.CMOD2 \tag{2}$$

$$T^{CMOD4} = \frac{0.75W_{CMOD4} + W_1}{A_{lig}}, \quad W_1 = \frac{0.75}{2}\left(\frac{S}{L}m_1 + 2m_2\right)g.CMOD4 \tag{3}$$

where,

A_{lig} : ligament area (mm^2)
S : loading span (mm)
L : length of specimen (mm)
m_1 : mass of specimen (kg)
m_2 : mass of equipment that follows the beam until failure
g : 9.807 m/s^2
$CMOD_c$: CMOD until specimen breaks
CMOD2 : 0.02D
CMOD4 : 0.04D

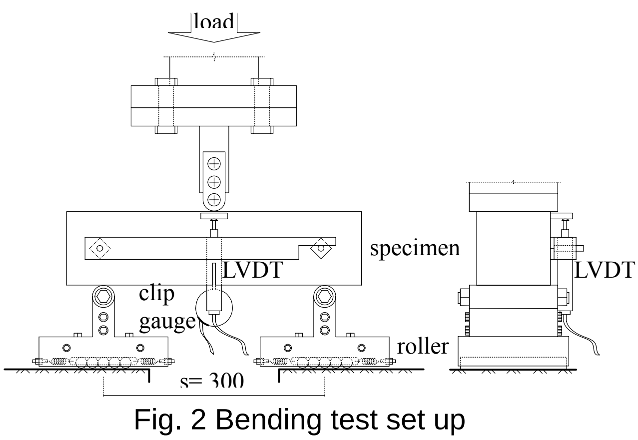

Fig. 2 Bending test set up

3. RESULTS AND DISCUSSIONS

3.1 General properties

Fresh and hardened properties of each concrete series are shown in Table 3 and Table 4, respectively. No significant difference is noticed among the data. Better compaction and lesser air content on P6 series might be the factors causing this particular series to have higher compressive strength compared to Hybrid series.

Table 3 Fresh properties

I.D.	Slump (mm)	Air content (%)
Plain	210	3.5
P6	200	2.2
Hy1	120	2.9
Hy2	200	3.0

Table 4 Hardened properties

I.D.	Density (kg/m^3)	UPV (km/s)	f_{cu} (MPa)	E (GPa)
Plain	2430	4.99	91.2	41.4
P6	2470	5.13	114.9	40.5
Hy1	2460	5.00	101.2	48.5
Hy2	2470	4.90	99.5	39.9

Mass loss of all series after heating is shown in Fig. 3. The difference in mass loss between Plain series and other series is found to represent the value of fiber volume fraction added inside the concrete mixture. In other words, almost all series contained approximately the same moisture content during testing.

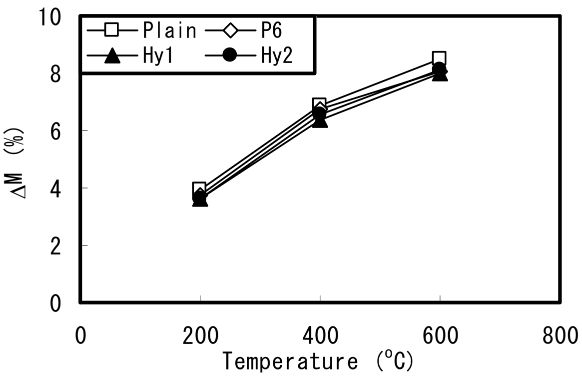

Fig. 3 Mass loss after heating

Significant deterioration in concrete properties is observed with respect to maximum heating temperature. Fig. 4 and Fig.5 shows the reduction in UPV and compressive strength. This trend is identical in all series.

In spite of its effectiveness in mitigating explosive spalling, melting of polypropylene fibers on P6 series might be considered as one factor (among others) causing significant deterioration in compressive strength. On the contrary, both Hybrid series shows lesser reduction rate up to 450 °C regardless of same amount of polypropylene fibers added into the concrete mixture as in P6 series. Beyond 600 °C, bond between steel fibers and concrete matrix was severely disrupted, leading to a higher reduction rate in compressive strength. Further, Hy2 series is found to have the capacity in maintaining residual compressive strength compared to Hy1 series. The effect of shorter steel fibers that was finely distributed inside concrete matrix might play a role causing this phenomenon.

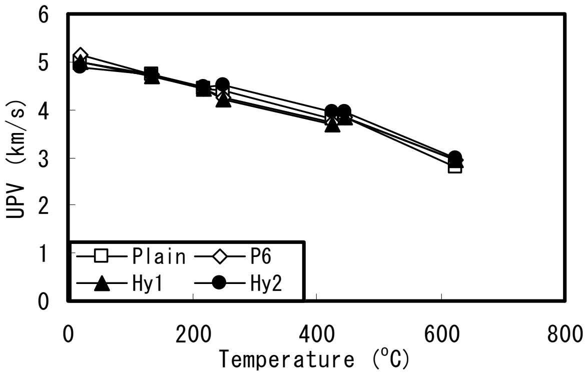

Fig. 4 Ultra pulse velocity vs. temperature

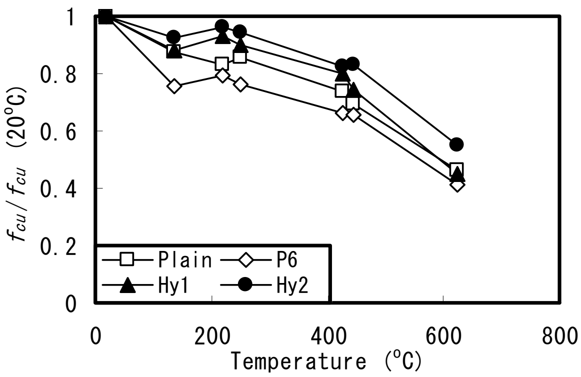

Fig. 5 Compressive strength vs. temperature

Regression analysis was performed to analyze the correlation between UPV and compressive strength of heated concrete [6]. The correlation, including all data series, is shown as thick line in Fig. 6 and can be represented as:

$$f_{cu} = 19.1e^{0.34v}\text{, giving } R^2=0.82 \tag{4}$$

where:

f_{cu} : compressive strength (MPa), cube

v : UPV (km/s)

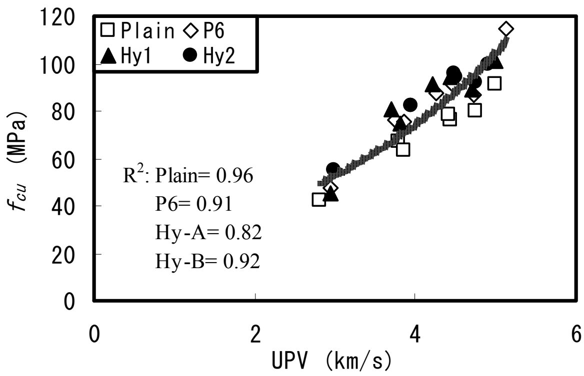

Fig. 6 Compressive strength vs. UPV

3.2 Fracture energy

L-CMOD curves of each series after particular heating temperatures: 20 (non-heated), 200, 400, and 600 °C are shown in Fig. 7 to Fig. 10. The curves are representation of specimens which yielded highest ultimate load (L_p) during the bending test.

Reduction in ultimate load is observed in all series with respect to maximum heating temperature, as summarized in Fig. 11. Beyond 200 °C, Plain series is found to have the highest reduction in ultimate load. The reduction may reach up to 50% after heating at 600 °C. On the contrary, increase in ultimate load is noticed on Plain and P6 series after heating at 200 °C. This phenomenon might be explained due to the fact that drying of concrete specimens yield to higher strength which encounters the negative effect of cracks after heating of specimens. At any particular heating temperature, ultimate load of Hybrid series is found to be higher compared to Plain and P6 series. However, reduction rate at the temperature range of 400 to 600 °C is found to be steeper than the one at the range of 200 to 400 °C for Hybrid series. As a consequence, this significant decrease in ultimate load will affect the value of residual G_F.

$CMOD_c$ of Plain and P6 series become longer with respect to maximum heating temperature, indicating ductile behavior. This ductile behavior was reported to be affected by thermal damage and drying of concrete causing more tortuous fractured surface [7] and may play an important role in affecting G_F value after heating. Little increase in residual G_F can be noticed after particular heating temperature as shown in Table 5.

Meanwhile, Hybrid series behaves differently compared to Plain and P6 series. The tail of L-CMOD curve on Hybrid series would not reach $CMOD_c$ soon after the ultimate load. Load decreases gradually with respect to increase in CMOD. The main reason for this is believed to correspond with the crack-arresting and crack-bridging mechanism of steel fibers. Improvement in residual G_F is achieved through these mechanisms inside the concrete matrix. However, further disruption of transition zone between steel fibers and concrete matrix after heating at 600 °C caused reduction in ultimate load, affecting overall fracture behavior performance of Hybrid series.

Fig. 12 shows G_F values of all series after heating. Like reported elsewhere, G_F value of some series increases with increasing heating temperature and decreases beyond particular transition point of temperature [7]. It is worth notice that for Plain and P6 series, the tail of L-CMOD curve behavior is the main factor increasing G_F value rather than the ultimate load. Meanwhile, residual G_F of Hybrid series decreases with respect to maximum heating temperature, especially after maximum heating temperature of 200 °C.

Apparently, it is obvious that inclusion of steel fibers significantly improved residual G_F value through crack-arresting and crack-bridging mechanism. Fixing Plain series as control specimen, residual G_F of Hybrid series is calculated to be approximately 5 times than control residual G_F after heating at 200 and 400 °C. After heating at 600 °C, the value reduces to 2.25. All comparison on Hybrid series is performed on T^{CMOD2} value, as shown in Fig. 13.

Table 5 Ultimate load and fracture energy

<table>
<tr><th colspan="2">I.D.</th><th>L_p (N)</th><th>G_F (N/m)</th><th>T^{CMOD2} (N/m)</th><th>T^{CMOD4} (N/m)</th></tr>
<tr><td rowspan="4">Plain</td><td>20C</td><td>4567</td><td>96.2</td><td rowspan="8" colspan="2">–</td></tr>
<tr><td>200C</td><td>4594</td><td>105.8</td></tr>
<tr><td>400C</td><td>3207</td><td>90.6</td></tr>
<tr><td>600C</td><td>2263</td><td>107.3</td></tr>
<tr><td rowspan="4">P6</td><td>20C</td><td>4199</td><td>90.7</td></tr>
<tr><td>200C</td><td>4868</td><td>121.2</td></tr>
<tr><td>400C</td><td>4446</td><td>144.3</td></tr>
<tr><td>600C</td><td>3468</td><td>121.6</td></tr>
<tr><td rowspan="4">Hy1</td><td>20C</td><td>5377</td><td rowspan="8">–</td><td>549.6</td><td>884.7</td></tr>
<tr><td>200C</td><td>5277</td><td>475.2</td><td>793.5</td></tr>
<tr><td>400C</td><td>4694</td><td>457.0</td><td>698.6</td></tr>
<tr><td>600C</td><td>3073</td><td>206.6</td><td>264.8</td></tr>
<tr><td rowspan="4">Hy2</td><td>20C</td><td>5377</td><td>486.4</td><td>749.6</td></tr>
<tr><td>200C</td><td>5504</td><td>560.5</td><td>907.0</td></tr>
<tr><td>400C</td><td>4962</td><td>437.1</td><td>676.5</td></tr>
<tr><td>600C</td><td>3026</td><td>283.5</td><td>384.1</td></tr>
</table>

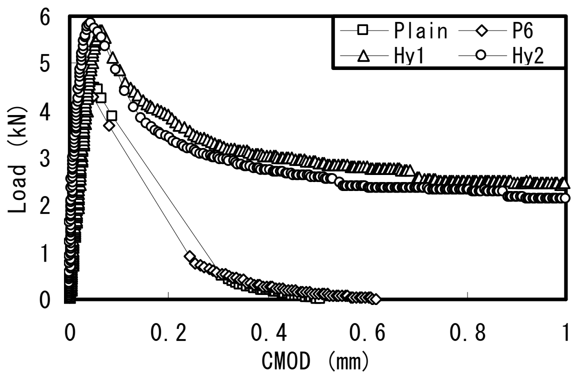

Fig. 7 L-CMOD at 20 °C

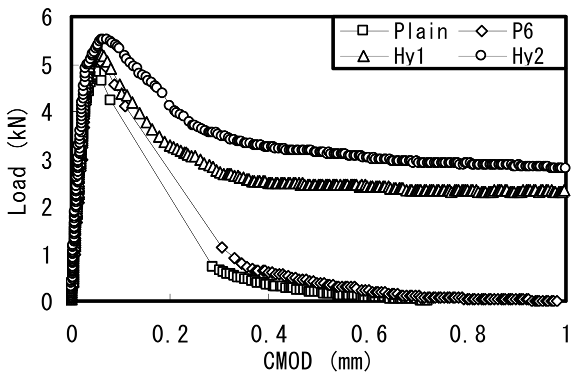

Fig. 8 L-CMOD at 200 °C

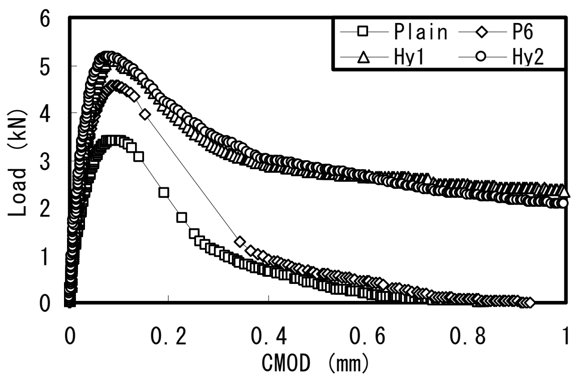

Fig. 9 L-CMOD at 400 °C

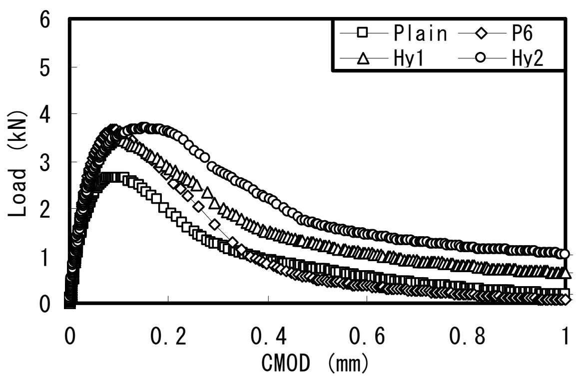

Fig. 10 L-CMOD at 600 °C

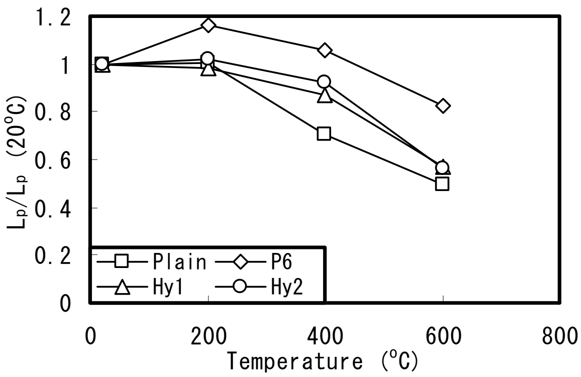

Fig. 11 Ultimate load vs. temperature

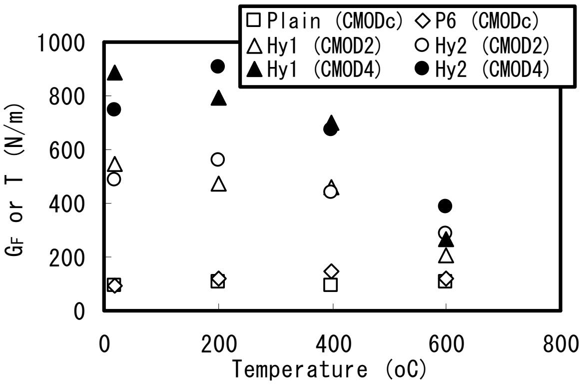

Fig. 12 Fracture energy vs. temperature

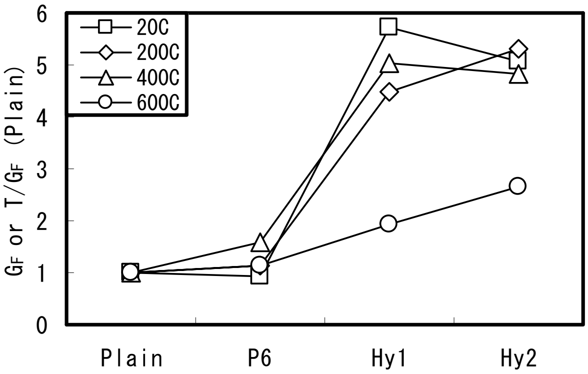

Fig. 13 Relative G_F with respect to G_F Plain

5. CONCLUSIONS

(1) Correlation between UPV and compressive strength of heated concrete specimen yield to a good agreement. Implementation of this method will help the assessment of fire damaged concrete to be more practical and efficient.

(2) Ultimate load decreases with respect to maximum heating temperature. Among all the series investigated, Plain series is found to have the highest reduction in ultimate load.

(3) Ultimate load reduction rate of Hybrid series is found to be steeper in the temperature range of 400-600 °C. At this temperature range, further disruption of bond between steel fibers and concrete matrix is believed to reduce the effectiveness of steel fibers in arresting and bridging the cracks upon loading. As a consequence, overall fracture performance of Hybrid series reduces.

(4) Improvement in residual G_F is achieved through crack-arresting and crack-bridging mechanism of steel fibers inside the concrete matrix of Hybrid series.

(5) Hybrid fiber systems significantly improved residual G_F value. Ratio of residual G_F of Hybrid series (calculated based on T^{CMOD2}) to Plain series reaches 5 after heating at both 200 and 400 °C

REFERENCES

[1] Castillo, C. and Durrani, A.J., "Effect of Transient High Temperature on High-Strength Concrete", ACI Materials Journal, Vol. 87, Jan. 1990, pp. 47-53

[2] Phan, L.T., Lawson, J.R., Davis, F.L., "Effects of Elevated Temperature Exposure on Heating Characteristics, Spalling, and Residual Properties of High Performance Concrete," Materials and Structures, Vol. 34, Mar. 2001, pp. 83-91

[3] Bilodeau, A., Malhotra, V.M., and Hoff, G.C., "Hydrocarbon Fire Resistance of High Strength Normal Weight and Light Weight Concrete Incorporating Polypropylene Fibers," International Symposium on High Performance and Reactive Powder Concretes, 1998, pp. 271-296

[4] Suhaendi, S.L., Sudo, M., and Horiguchi T., "Optimization of polypropylene fibers for high strength concrete under high temperature condition," Proceedings of EASEC-10, Vol.6, 2006, pp. 467-472

[5] Gopalaratnam, V.S., "On the characterization of flexural toughness in fiber reinforced concretes," Cement and Concrete Composites, Vol. 17, 1995, pp. 239-254

[6] Suhaendi, S.L., and Horiguchi, T., "Effect of short fibers on residual permeability and mechanical properties of hybrid fiber-reinforced high-strength concrete after heat exposition," Cement and Concrete Research, Vol. 36, 2006, pp. 1672-1678

[7] Nielsen, C.V., and Bićanić, N., "Residual fracture energy of high performance and normal concrete subject to high temperatures," Materials and Structures, Vol. 36, 2003, pp. 515-521